Original Article

The association between genomic variations and histological grade in hepatocellular carcinoma

Jun Liu[1], Guangbing Li[1], Yuan Guo[2], Ning Fan[2], Yunjin Zang[2]

[1]Department of Hepatobiliary Surgery and Liver Transplantation, Shandong Provincial Hospital Affiliated to Shandong University, Jinan 250021, China; [2]Organ Transplant Center, the Affiliated Hospital of Qingdao University, Qingdao 266000, China

Contributions: (I) Conception and design: Y Zang; (II) Administrative support: Y Zang; (III) Provision of study materials or patients: All authors; (IV) Collection and assembly of data: All authors; (V) Data analysis and interpretation: J Liu; (VI) Manuscript writing: All authors; (VII) Final approval of manuscript: All authors.

Correspondence to: Yunjin Zang. Organ Transplant Center, the Affiliated Hospital of Qingdao University, Qingdao 266000, China. Email: zangyj3657@qq.com.

Background: Histological grade (HG) is an important prognostic factor for hepatocellular carcinoma. With the development of precision medicine, diagnosis with a sequencing technology has become increasingly accepted. It is vital to discuss their similarities and differences to bridge or improve the traditional HG diagnosis with the novel sequencing technique.

Methods: A total of 658 tumor samples were collected from 602 Chinese hepatocellular carcinoma patients and sequenced for a panel of pan-cancer genes. Nucleotide usage bias, genomic variation-related scores, driver genes, and biological processes were compared among different HGs. These results were further verified using a cohort dataset from the Western population.

Results: Genomic variation subtypes, such as C>G substitution, maximum somatic allele frequency (MSAF), and *TP53*, and biological processes including "angiogenesis" and "regulation of homotypic cell-cell adhesion" were found to be significantly associated with HG in both Chinese and Western populations.

Conclusions: The association identified between genomic variation and HG could aid our understanding of HG as an important clinical measure, and potentially be used to predict HG for hepatocellular carcinoma.

Keywords: Histological grade (HG); hepatocellular carcinoma; sequencing; genomic variation

Submitted Oct 29, 2019. Accepted for publication Feb 17, 2020.
doi: 10.21037/tcr.2020.03.32
View this article at: http://dx.doi.org/10.21037/tcr.2020.03.32

Introduction

Histological grade (HG) describes the aggressive potential of solid tumors. The classical and widely adopted grading system for hepatocellular carcinoma is Edmondson-Steiner (ES), which is based on microscopic evaluation of the tubule formation, mitotic count, and nuclear pleomorphism. According to the ES grading system, tumors can be classified into three or four grades. A tumor of a higher grade tends to grow and spread at a faster pace, which needs more urgent and aggressive treatment.

Needle biopsies and histopathological evaluation works as a gold standard for HG diagnosis. Collectively, clinical physicians have accumulated a large amount of experience in using this method. However, it has two major problems, diagnostic subjectivity and biopsy inaccessibility (1), which might hinder its full efficacy. A stricter tumor grading requires two or more pathologists with expertise in a specific cancer to reduce diagnostic subjectivity. Much effort has been made with non-invasive methods such as magnetic resonance and contrast computed tomography (CT) to avoid biopsy unavailability (2). In contrast to diverse imaging methods, molecular biomarkers could overcome the two problems mentioned above. For example, miR-1290 could work as a biomarker of high-grade serous ovarian carcinoma (3), and tumor tissue protein signatures could predict the HG of breast cancer (4). Apart from the expression of biomarkers as an indicator

of HG, the genomic variation could also be used. Many gene mutations have been recognized to be associated with HG, such as TP53 (5), IDH1/2 (6) and ACVR2 (7). We are interested to know how far genomic variations are associated with HG in HCC because it can help us to understand HG as an important clinical measure.

With the development of precision medicine, DNA sequencing provides rich information for disease diagnosis and precision treatment. By using a liquid biopsy, genomic variations could prove to be more useful in predicting HG and could perfectly overcome the two major problems in the traditional ES grading system. Additionally, this method could provide necessary information for precise treatment in one-shot sequencing. However, ctDNA concentration is more easily affected by cancer development and clinical therapy, and the standard to detect ctDNA from liquid biopsy has not been well established.

This study sequenced 487 tissue samples from 459 Chinese HCC patients to build a solid connection between genomic variation and HG. Genomic variation, including nucleotide substitution/indel, truncation, gene homozygous deletion and fusion, were called. Association of HG with factors including genomic variation types, substitution types, mutational frequency related scores and biological processes was studied. Among the factors, those found to be significant were compared to those of the Western population.

Methods

Patients and samples

This study was approved by Shandong Provincial Hospital Affiliated to Shandong University and The Affiliated Hospital of Qingdao University. A total of 602 patients were enrolled. Each participant provided written informed consent. Samples were collected from surgery after diagnosis or relapse. HG was scored by a specialist in hepatobiliary pathology according to the Edmondson and Steiner method (8). Grade 1 was defined as well differentiated (WD), grade 2 and 3 as moderate differentiated (MD), grade 4 as poor differentiated (PD). The patients were staged according to the seventh edition of the tumor-node-metastasis (TNM) classification system for lung cancer from the American Joint Committee. We also collected another public dataset to validate our analysis. This dataset, MSKCC, containing 360 samples, was downloaded from cBioportal (https://www.cbioportal.org/, accessed on March 5, 2019).

Library preparation and next-generation sequencing

Tissue samples (40 μm section) were collected for each patient. KAPA Hyper Prep Kit (#07962363001, Roche, Basel, Switzerland) was used to extract DNA. PBS (phosphate-buffered saline) was added to those samples with volumes of less than 5 mL in order to make each sample volume equivalent to 5 mL. They were centrifuged (2 times at 1,600 g for 10 and 15 min, respectively) for extraction of DNA and the supernatant was separated. Invitrogen Qubit® DNA HS Assay Kit (#Q32854) was used to measure the DNA concentration. Single strand DNA and protein contamination were excluded. Library construction was only applied in samples with at least 50 ng of double-stranded DNA extracted. Molecular identifiers (MIDs) were added to the DNA segment ends for DNA libraries to reduce the false discovery rate (FDR). Barcodes were also added to the reads for multiplex sequencing. Sequencing was performed on an Illumina Novaseq 6000 (Illumina, San Diego, CA) for 151 bp read length from both ends. The average sequencing depth was about 3,000×.

Variants calling

A pan-cancer panel (Yuansuo®, Origimed, Shanghai, China) comprising 588 genes was captured with targeted amplification. Adaptors were trimmed from raw DNA reads by cutadapt (version 1.18) (9). MID-labeled reads were de-duplicated with an in-house pipeline. BWA MEM (version 0.7.9a) (10) mapped the high-quality reads to the UCSC hg19 reference sequences. Base quality was recalibrated by the BaseRecalibrator tool from GATK (version 3.8) (11). Mutect2 with a tumor-only mode (12) and Varscan (version 2.3.9) (13) with the default parameters were used to call variants.

For each sample, the germline variants having variant allele frequency (VAF) <0.1% were filtered according to the databases of ExAC (14), gnomAD (15), 1000 Genomes (16), and ESP6500 (17). Somatic variants that had not been filtered were further annotated by ANNOVAR (2017/07/17) (18) with RefSeq (version 2017/06/01).

Fermi-lite (19) was used to identify gene fusion and rearrangement. The breakpoints were further checked by BLAT (http://genome.ucsc.edu, version 3.50). Those reads uniquely mapping to the reference genome constituted rearrangement supported reads.

CNVKit (20) was used to estimate the logR scores. Copy number was assigned 1 for logR values below –0.25, 3 for

logR values above 0.25, and 2 for logR values in between –0.25 and 0.25 (21).

Bioinformatics analysis

The mutant allele tumor heterogeneity (MATH) score for a tumor was calculated as the median absolute deviation divided by the median MAF of all somatic mutations detected in the tumor sample. As suggested by Jiang *et al.* (22), the calculation of MATH used somatic mutation calls with MAF of 0.075 or greater. Clonal mutation burden (CMB) (22) was defined as the number of mutations per clone, and divided into low (low TMB, high MATH), high (high TMB, low MATH), or intermediate (others).

Statistical analysis

The Mann-Whitney U test was used to compare TMB, MSAF, MATH, and CMB between different HGs. Fisher's exact test was performed to compare the count number of nucleotide mutations for different HGs.

Survival analysis was conducted with R software. Samples were classified by a cutoff at the median mutational frequency. The survival time was plotted against overall survival probability by the Kaplan-Meier method. The log-rank test was applied to calculate the P value between the two groups.

Results

Patients and genomic variation detection

The analysis workflow of this study is illustrated in *Figure S1*. Initially, a total of 602 patients were enrolled in this study. Of these, only 459 patients had histological grading information available. The other patients' samples were thus filtered out from the following study. Their clinicopathologic characteristics are summarized in *Table S1*. The median age of patients was 55 years old (range, 16 to 82 years old). Most of the patients were male (87.6%). According to the TNM classification system (23), the number of patients in the early stage (I/II/III) and late-stage (IV) were 418 and 41, respectively. Patients who consumed alcohol more than 200 days per year were classified as "drinking", and those who had an immediate family member with any type of cancer were labeled as "family history". HGs were divided into three categories: poorly differentiated (PD), moderately differentiated (MD) and well differentiated (WD).

Tissue samples were prepared by surgery and enriched with a pan-cancer panel of genes (Yuansuo®, Origimed Co., Ltd, Shanghai, China) (*Figure S2*). For the 459 patients, 487 samples were collected. Somatic genomic variations (SGVs) were called by Mutec2 (12) and Varscan (13) for each sample. Gene amplifications were called by CNVKit (20). Fermi-lite (19) was used to identify gene fusion and rearrangement. The genomic variations at top high frequency are depicted in *Figure 1*. Genomic variations from multiple samples of each patient were merged under the same patient.

The bias of SGV types in different HGs

There are multiple types of SGVs deriving from different mechanisms. Those SGVs were classified into five types (fusion/rearrangement, gene amplification, gene homozygous deletion, substitution/indel, and truncation). The percentage of those groups was summarized according to the HG groups (*Figure 2A*). From poorly to moderately to well-differentiated HG, the percentage of the truncation and substitution/indel group increased but that of the gene amplification group dropped. The poorly differentiated group had the lowest percentage of fusion/rearrangement but the highest percentage of gene amplification variations.

Single nucleotide variants (SNVs) can be classified into transversion substitution and transition substitution. Transition SNVs regularly had a higher frequency and caused no functional change because of codon "wobble". To study the association between amino acid changes and HGs, the percentages of transversion and transition were compared (*Figure 2A*). In total, the percentage range of transversion and transition for different HGs was 65–72% and 28–34%, respectively. WD had higher transition than PD with percentages of 52% and 47%, respectively (P value =2.537e-11), but had lower transversion than PD with percentages of 48% and 53%, respectively (P value =2.2e-16). For specific substitutions, WD had less C>G transversion (P value =0.0058) and more G>A transition (P value =0.026) than non-WD. PD had higher C>T transition (P value =0.01) than non-PD.

Except for mutational occurrence, we also studied the association between HGs and mutational frequency related scores including maximum somatic allele frequency (MSAF) (24), MATH and CMB (22). MSAF was regularly used as a measure of cellular tumor prevalence. Higher MSAF denoted higher tumor content. The MATH score denoted allele heterogeneity among each sample, which reflected the diversity of mutational clones. CMB score combined

Figure 1 The landscape of genomic variations. From top to bottom, the bar plot indicates the tumor mutation burdens (TMBs) and the below heat map indicated the clinicopathological characteristics. HG (histological grades) includes WD (well-differentiated), MD (moderately differentiated), and PD (poorly differentiated). The bottom left bar plot indicates the percentage of genomic variation for each gene in the patients. The bottom right heatmap shows genomic variation types.

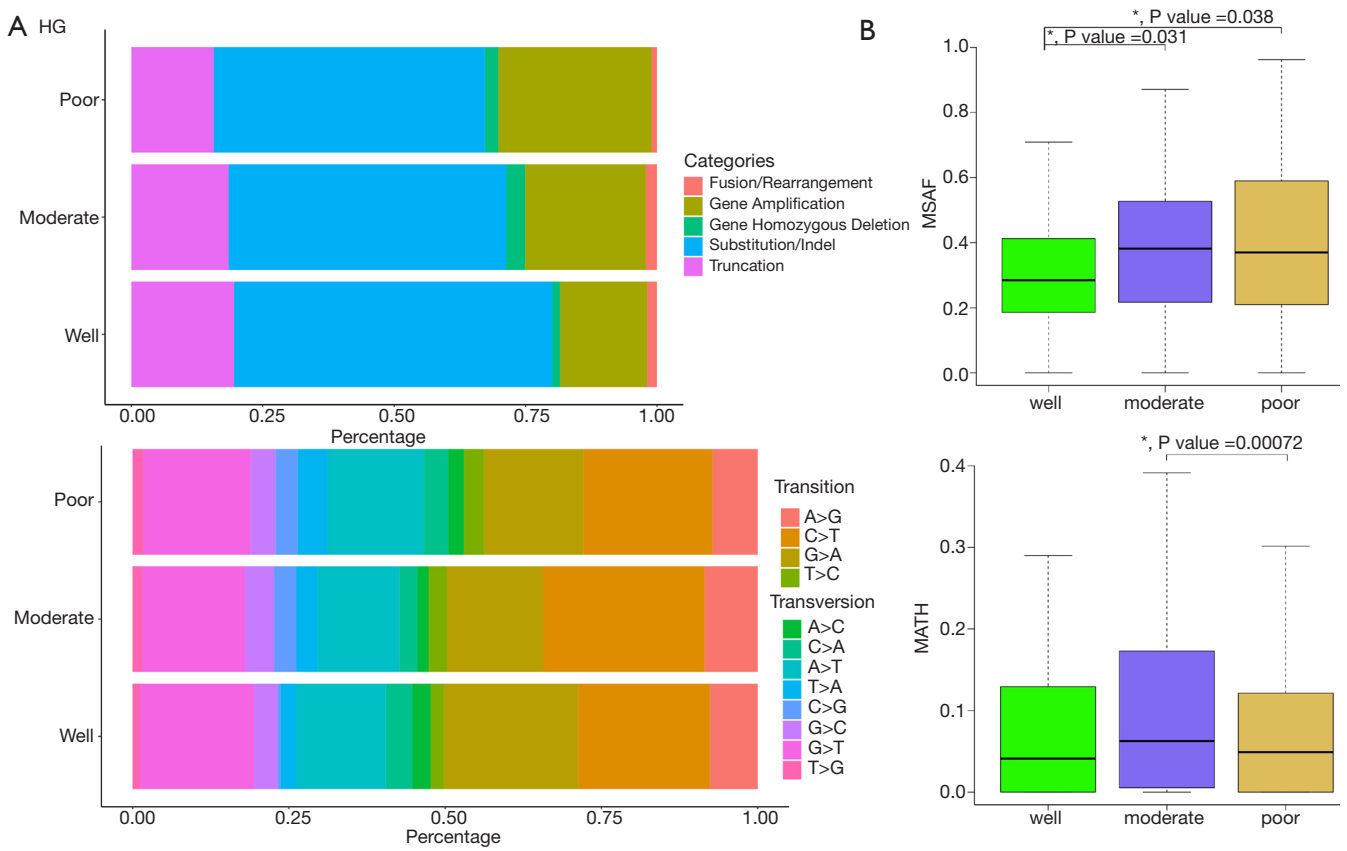

Figure 2 Variation distribution for hepatocellular carcinoma (HCC). (A) The upper plot shows the distribution of five types of genomic variation for three groups of HGs (histological grades). The lower plot is the distribution of 12 substitution types, which are grouped into transition and transversion. The x-axis indicates the patient percentage and the y-axis indicated the HGs. (B) The upper and the lower plots show MSAF (maximum somatic allele frequency) and MATH (mutant allele tumor heterogeneity) distributions for the three HG groups, respectively.

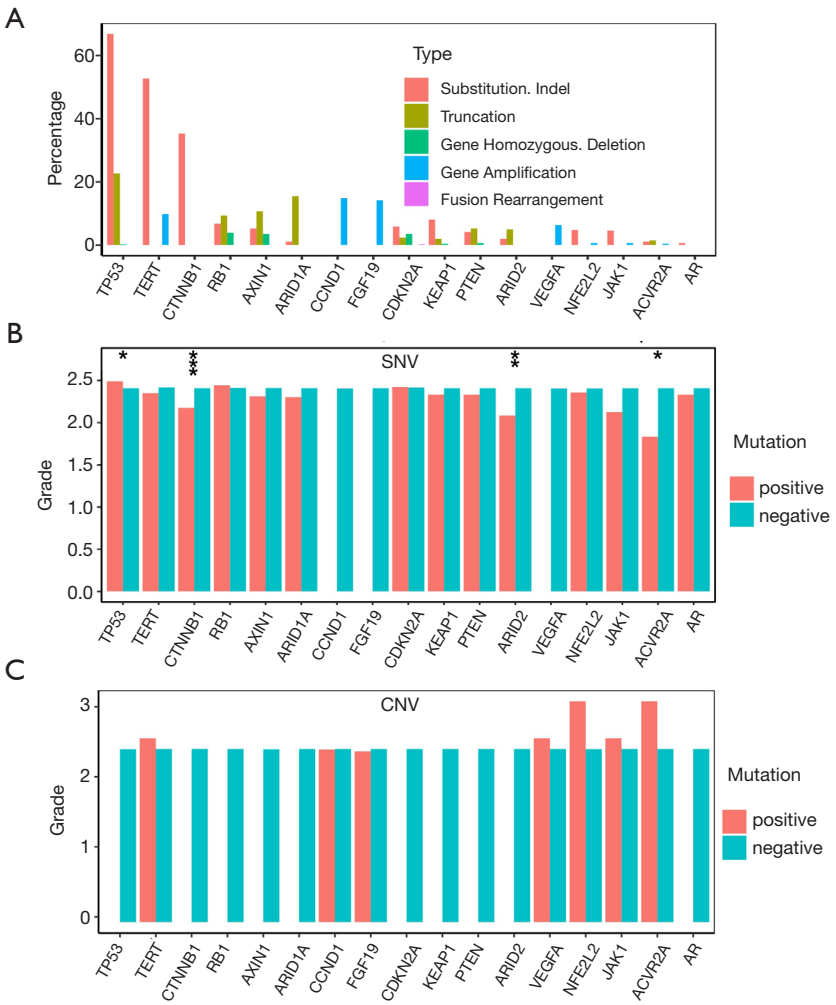

Figure 3 Frequency of genomic variation in driver genes. (A) The percentage of patients with five types of genomic variations for hepatocellular carcinoma (HCC) driver genes. (B) The average grade of tumors with/without substitution/indel/truncation mutations in driver genes. *, P<0.05; **, P<0.01; ***, P<0.001. (C) The average grade of tumors with/without amplification in driver genes. SNV, single-nucleotide variant; CNV, copy number variation.

the tumor mutation burden (TMB) and MATH score (22). High CMB was defined as high TMB and low MATH. These scores were compared among different HGs. WD had significantly lower MSAF than MD and PD with P values equal to 0.031 and 0.038, respectively (*Figure 2B*). As for the MATH score, MD was highest among HGs, but only MD transversion. PD had a P value of less than 0.05. We also tested the CMB score, but no significant difference was found among HGs (result not shown).

The functional bias of genomic variations for different HGs

Driver genes play a big part in cancer. Their specific effect on HG was also studied. The driver genes of HCC were collected from the literature (25,26). The top 10 variable genes are displayed in *Figure 3A*. Genes *TP53*, *TERT*, *CTNNB1*, *RB1*, *AXIN1*, and *ARID1A* were prone to substitution/indel/truncation variation, while *CCND1*, *FGF19*, *FGF4*, and *FGF3* preferred gene amplification. Among those driver genes, there were three genes showing significantly different HGs after mutation (*Figure 3B*). Of these three genes, mutational *TP53* (*TP53*$^{+}$) had a higher average HG than non-mutational *TP53* (*TP53*$^{-}$). A non-parameter Wilcoxon's rank-sum test showed significance at P value =3.8e-2. In contrast, mutational *CTNNB1* (*CTNNB1*$^{+}$) and *FGF3* (*FGF3*$^{+}$) showed significantly lower

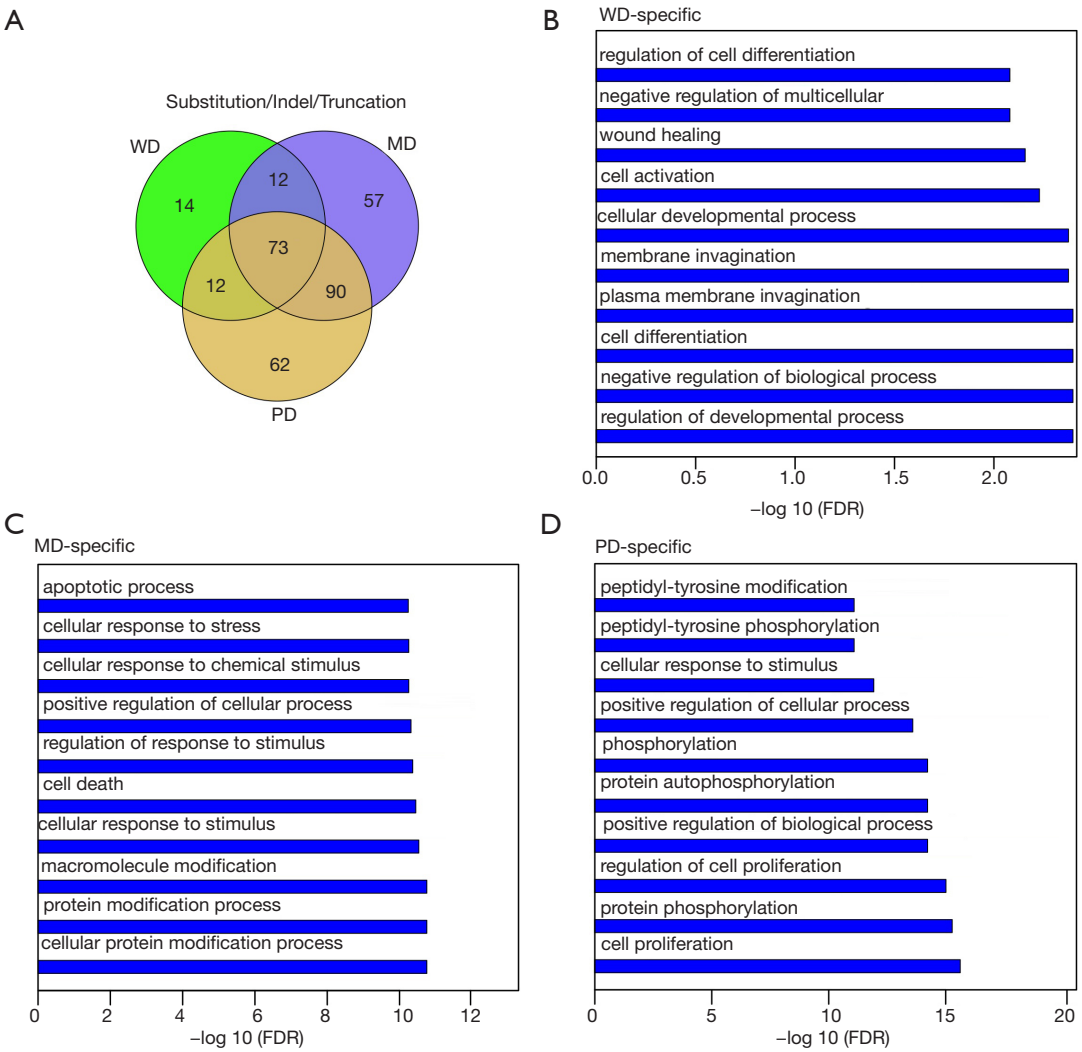

Figure 4 The substitution/indel/truncation overlaps between different histological grades. (A) The substitution/indel/truncation overlaps between three HGs including WD, MD, and PD; (B) the enriched biological processes for well-differentiated tumors; (C) the enriched biological processes for moderately differentiated tumors; (D) the enriched biological processes for poorly differentiated tumors. The length of the blue bar indicates the negative log-transformed false discovery rate (FDR). HGs, histological grades; WD, well-differentiated; MD, moderately differentiated; PD, poorly differentiated.

HG with P value =7.8e-4 and P value =0.04, respectively. We also tested the association between gene amplification variation and HG for those driver genes, but no significant difference was found (*Figure 3C*).

Mutations, such as substitution, indel, and truncation, can modify the targeted gene functions, and amplification can modify their expression. To study their functional bias, three HG groups were intersected with each other as displayed by a Venn plot in *Figure 4A*. WD, MD, and PD had 14, 57 and 62 unique mutated genes, respectively. WD had fewer unique mutated genes than other HGs. The unique genes for WD and PD were enriched with the biological processes of gene ontology. A hypergeometric test was performed for each biological process. The Bonferroni-Hochberg (BH) method was applied to correct for multiple testing errors. The top 10 enriched biological processes are listed in *Figure 4B,C,D*. WD was enriched in the regulation of the developmental process, cell differentiation, and membrane invagination. There were 1,168 biological processes enriched for PD specific mutations with multiple testing corrected P values less than 0.05, such as cell proliferation, protein phosphorylation,

and cellular response to a stimulus.

Apart from substitution/indel/truncation mutations, copy number variation can also disrupt cellular function by modifying gene regulation. The amplified genes were intersected with each other (*Figure S3A*) to obtain the HG-specific genes. The specific genes had similar distribution as substitution/indel/truncation for gene amplification. WD had less specific gene amplification than other HGs, while PD had the highest number of specific genes. WD was enriched in the regulation of fibroblast migration and the negative regulation of transport (*Figure S3B*); MD was enriched in the positive regulation of cellular processes and the regulation of cell proliferation (*Figure S3C*); and PD was enriched in the positive regulation of metabolic processes (*Figure S3D*).

Comparison to the Western population

The findings above were compared against the Western population. An MSKCC dataset from the Western population was downloaded from cBioportal (https://www.cbioportal.org/, accessed on March 5, 2019). With this dataset, nucleotide usage, TMB, driver genes, and biological processes were analyzed using the same procedures as in our dataset. Results showed that WD possessed a higher percentage of transition mutation than PD in the Western population. Meanwhile, PD held a higher percentage of transversion than WD. Such results were in line with those from our dataset. As for the nucleotide usage, only C>G transversion showed higher frequency in PD than in WD (P value =0.017), matching the result from our dataset. Specifically to the Western population, WD had higher A>G mutation than non-WD with P value =0.031. PD had higher A>C and lower A>G substitution than non-PD with P values =0.036 and 7.5e-4, respectively. Among the driver genes, only TP53 mutation was consistently associated with higher HG (P value =1.3e-3, Mann-Whitney U test). Additionally in the Western population, the RB1 mutation tended to be enriched in the high-grade samples.

Further investigation of the similarity between the functional biases for WD- and PD-specific genes revealed an extraordinary consistency. The top significantly enriched biological processes in our dataset showed similar significance in the MSKCC dataset (*Figure 5A,B,C*). For example, for both our dataset and the MSKCC dataset, PD-specific genes took part in cell proliferation, protein phosphorylation, and regulation of cell proliferation; MD-specific genes took part in the cellular protein modification process and cellular response to stimulus; and WD-specific genes taking part in the regulation of developmental processes and cell differentiation.

It was noteworthy that HG-specific genes may share common enriched biological processes (*Figure 5D*). To extract the consistent HG-specific biological processes between the two datasets, we first extracted the HG-specific biological processes taken by HG-specific genes for both datasets. Then an intersection was conducted between HG-specific biological processes for both datasets. Through these means, we identified the HG-specific biological processes commonly taken by both datasets. There were 3 WD-specific, 150 MD-specific and 64 PD-specific common biological processes (*Table S2*). These gene lists were applied for gene ontology enrichment analysis. The PD-specific common biological processes included angiogenesis, phosphatidylinositol-3-phosphate biosynthetic process, glycerophospholipid metabolic process and development of primary male sexual characteristics; the MD-specific common biological processes included response to hydrogen peroxide, response to peptide hormone and protein localization to the nucleus; and the three WD-specific common biological processes were regulation of epithelial to mesenchymal transition involved in endocardial cushion formations, epithelial to mesenchymal transition involved in endocardial cushion formations and regulation of homotypic cell-cell adhesion.

Discussion

Although there have been many studies on the association between gene expression and HG, information on the association between genomic variation and HG is still scarce. The intention of this study was to understand the association between genomic variation and HG and explore the potential of genomic variation as an indicator of HG.

A stable genomic variation pattern should be associated with a hidden molecular mechanism. For example, C>T and C>G substitution could come from DNA editing catalyzed by apolipoprotein B mRNA catalytic subunit-like (APOBEC) and activation-induced deaminase (AID) family, which can bind to both RNA and single-stranded (ss) DNA. DNA deamination by these proteins results in the C>U conversion in single-stranded DNA. Such mutations could result in C>T transition and C>G transversion by different DNA repair polymerases (27). In lung cancer, different cancer subtypes also showed a large difference in C>T transition and C>G transversion (28). Due to the existence

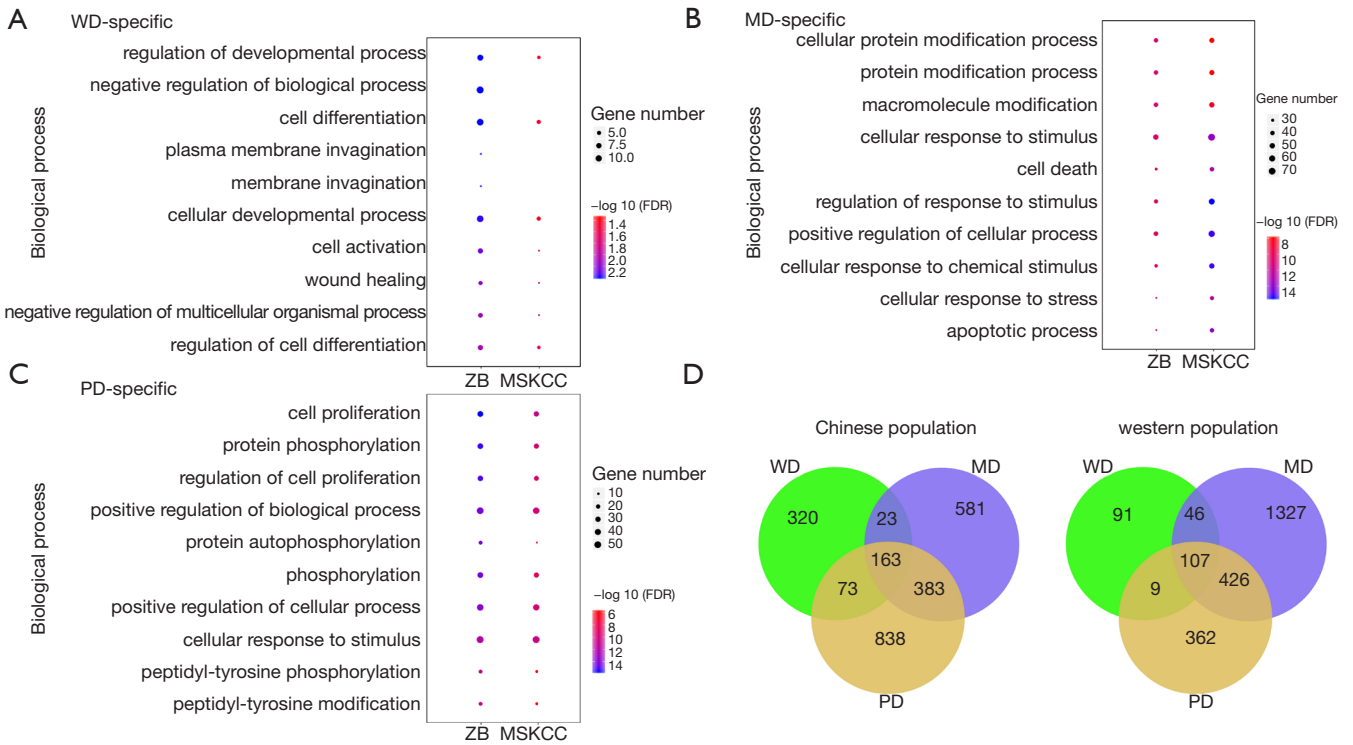

Figure 5 Biological processes could predict survival accurately. (A) The top enriched biological process in WD-specific genes from the Chinese population was validated in the Western population; (B) the top enriched biological process in MD-specific genes from the Chinese population was validated in the Western population; (C) the top enriched biological process in PD-specific genes from the Chinese population was validated in the Western population; (D) the intersection of enriched biological processed in the Chinese population and the Western population. WD, well-differentiated; MD, moderately differentiated; PD, poorly differentiated.

of such molecular mechanisms, those stable genomic variation patterns could be stable predictors of HG. In this study, we have analyzed the association of HGs with genomic variation and mutational frequency in the Chinese population and the Western population, and have found a higher C>G transversion mutated in patients with PD HCC for both populations. This association was meaningful in the treatment of such a subset of HCC patients. As reported, APOBEC-related mutagenesis was found to be highly correlated with immunotherapy response (29). Thus, detected C>G transversion could be a good indicator of immunotherapy efficacy. In spite of high C>G transversion being found in HCC and believed as an etiology of HCC by Morishita *et al.* (30), they did not associate it with any biological significance. Our results revealed that patients with high C>G transversion were strongly associated with poorly differentiated HCC, involving in APOBEC-related mutagenesis.

Taking into account the important mutational scores in relation to survival, we also studied TMB, MSAF, MATH and CMB score, among which only MSAF is significantly associated with HG. As a measure of cellular tumor prevalence, MSAF has been used in many studies (24,31,32). Studies have shown that MSAF is also correlated with tumor burden (31) and several other research studies have revealed that tumor burden is strongly associated with HG (32). Therefore, it is reasonable that MSAF was significantly associated with HG.

Among the driver genes of HCC, *TP53* mutation was a consistent biomarker of high HG in both populations, which agreed with the previous studies in ovarian cancer (5) and HCC (33). However, we also noticed difference between the Chinese and Western populations. In the Chinese population, mutations in *CTNNB1*, *ARID2*, and *ACVR2A* were associated with a lower HG, and in the western population, *RB1* was associated with a high HG.

During the analysis of biological processes of substitution/indel/truncation and amplification for WD- and PD-specific genes, we found that the biological

processes were highly matched for mutation and amplification. For example, WD tumors showed higher substitution/indel/truncation and amplification in the cell differentiation, and PD tumor showed higher substitution/indel/truncation and amplification in the protein phosphorylation. These results demonstrated that a tumor could become WD or PD either through mutations or by amplification, or both. Comparisons between the Chinese and the Western populations also proved that the WD was most enriched in cell differentiation, and the PD was most enriched in phosphorylation. Furthermore, there were also genes for WD or PD involved in phosphorylation or cell differentiation, respectively. A further intersection of their biological processes disclosed the unique biological processes for different HGs. Although these biological processes have been well recognized in basic cancer research, they have not been systematically associated with genomic variations and HG in HCC before.

It should be noted that, instead of ctDNA (circulating tumor DNA) from blood, DNA from the solid tumor was extracted to detect gene mutations. Considering the instability of ctDNA detection, this should be a very important step for applying genomic variations as a predictor of HG. For example, ctDNA is easier to be detected in late-stage cancer and its concentration can be changed by many factors including clinical therapy and tumor development. How the instability of ctDNA detection affects its prediction is another issue to be discussed. The other limitation of this study is that the comparison with the Western population did not include CNV due to the missing information in the MSKCC dataset.

In summary, this pilot study has revealed multiple factors associated with HG. These findings improved our understanding of the molecular mechanism in different HGs of HCC. Further research using ctDNA to detect the genomic variation should be performed to verify this study.

Acknowledgments

Funding: None.

Footnote

Conflicts of Interest: All authors have completed the ICMJE uniform disclosure form (available at http://dx.doi.org/10.21037/tcr.2020.03.32). The work was carried out as part of the employment of the corresponding author at the Affiliated Hospital of Qingdao University. The Affiliated Hospital of Qingdao University was not involved in the manuscript writing, editing, approval, or decision to publish. The other authors have no conflicts of interest to declare.

Ethical Statement: The authors are accountable for all aspects of the work in ensuring that questions related to the accuracy or integrity of any part of the work are appropriately investigated and resolved. This study was approved by Shandong Provincial Hospital Affiliated to Shandong University and The Affiliated Hospital of Qingdao University. Each participant provided written informed consent. The study was conducted in accordance with the Declaration of Helsinki (as revised in 2013).

References

1. Cillo U, Giuliani T, Polacco M, et al. Prediction of hepatocellular carcinoma biological behavior in patient selection for liver transplantation. World J Gastroenterol 2016;22:232-52.
2. Schadendorf D, Hodi FS, Robert C, et al. Pooled Analysis of Long-Term Survival Data From Phase II and Phase III Trials of Ipilimumab in Unresectable or Metastatic Melanoma. J Clin Oncol 2015;33:1889-94.
3. Kobayashi M, Sawada K, Nakamura K, et al. Exosomal miR-1290 is a potential biomarker of high-grade serous ovarian carcinoma and can discriminate patients from those with malignancies of other histological types. J Ovarian Res 2018;11:81.
4. Skoog P, Ohlsson M, Ferno M, et al. Tumor tissue protein signatures reflect histological grade of breast cancer. PLoS One 2017;12:e0179775.
5. Cole AJ, Dwight T, Gill AJ, et al. Assessing mutant p53 in primary high-grade serous ovarian cancer using immunohistochemistry and massively parallel sequencing. Sci Rep 2016;6:26191.
6. Deng L, Xiong P, Luo Y, et al. Association between

IDH1/2 mutations and brain glioma grade. Oncol Lett 2018;16:5405-9.
7. Wodziński D, Wosiak A, Pietrzak J, et al. Does the expression of the ACVR2A gene affect the development of colorectal cancer? Genet Mol Biol 2019;42:32-9.
8. Edmondson HA, Steiner PE. Primary carcinoma of the liver: a study of 100 cases among 48,900 necropsies. Cancer 1954;7:462-503.
9. Martin M. Cutadapt removes adapter sequences from high-throughput sequencing reads. EMBnet Journal 2011;17:3.
10. Li H, Durbin R. Fast and accurate short read alignment with Burrows-Wheeler transform. Bioinformatics 2009;25:1754-60.
11. McKenna A, Hanna M, Banks E, et al. The Genome Analysis Toolkit: a MapReduce framework for analyzing next-generation DNA sequencing data. Genome Res 2010;20:1297-303.
12. Cibulskis K, Lawrence MS, Carter SL, et al. point mutations in impure and heterogeneous cancer samples. Nat Biotechnol 2013;31:213-9.
13. Koboldt DC, Chen K, Wylie T, et al. VarScan: variant detection in massively parallel sequencing of individual and pooled samples. Bioinformatics 2009;25:2283-5.
14. Karczewski KJ, Weisburd B, Thomas B, et al. The ExAC browser: displaying reference data information from over 60 000 exomes. Nucleic Acids Res 2017;45:D840-D845.
15. Lek M, Karczewski KJ, Minikel EV, et al. Analysis of protein-coding genetic variation in 60,706 humans. Nature 2016;536:285-91.
16. 1000 Genomes Project Consortium, Abecasis GR, Altshuler D, et al. A map of human genome variation from population-scale sequencing. Nature 2010;467:1061-73.
17. NHLBI. Exome Variant Server. Available online: https://evs.gs.washington.edu. 2017/7/1.
18. Wang K, Li M, Hakonarson H. ANNOVAR: functional annotation of genetic variants from high-throughput sequencing data. Nucleic Acids Res 2010;38:e164.
19. Li H. FermiKit: assembly-based variant calling for Illumina resequencing data. Bioinformatics 2015;31:3694-6.
20. Talevich E, Shain AH, Botton T, et al. CNVkit: Genome-Wide Copy Number Detection and Visualization from Targeted DNA Sequencing. PLoS Comput Biol 2016;12:e1004873.
21. Murtaza M, Dawson SJ, Pogrebniak K, et al. Multifocal clonal evolution characterized using circulating tumour DNA in a case of metastatic breast cancer. Nat Commun 2015;6:8760.
22. Jiang T, Shi W, Wali VB, et al. Predictors of Chemosensitivity in Triple Negative Breast Cancer: An Integrated Genomic Analysis. PLoS Med 2016;13:e1002193.
23. Edge SB, Byrd D, Compton C, et al. Digestive system. In: Trotti A. editor. AJCC cancer staging manual, ed 7th. New York: Springer, 2010.
24. Schrock AB, Pavlick D, Klempner SJ, et al. Hybrid Capture-Based Genomic Profiling of Circulating Tumor DNA from Patients with Advanced Cancers of the Gastrointestinal Tract or Anus. Clin Cancer Res 2018;24:1881-90.
25. Lee JS. The mutational landscape of hepatocellular carcinoma. Clin Mol Hepatol 2015;21:220-9.
26. Ding XX, Zhu QG, Zhang SM, et al. Precision medicine for hepatocellular carcinoma: driver mutations and targeted therapy. Oncotarget 2017;8:55715-30.
27. Alexandrov LB, Nik-Zainal S, Wedge DC, et al. Signatures of mutational processes in human cancer. Nature 2013;500:415-21.
28. Kandoth C, McLellan MD, Vandin F, et al. Mutational landscape and significance across 12 major cancer types. Nature 2013;502:333-9.
29. Boichard A, Pham TV, Yeerna H, et al. APOBEC-related mutagenesis and neo-peptide hydrophobicity: implications for response to immunotherapy. Oncoimmunology 2018;8:1550341.
30. Morishita A, Iwama H, Fujihara S, et al. Targeted sequencing of cancer-associated genes in hepatocellular carcinoma using next-generation sequencing. Oncol Lett 2018;15:528-32.
31. Zhou C, Yuan Z, Ma W, et al. Clinical utility of tumor genomic profiling in patients with high plasma circulating tumor DNA burden or metabolically active tumors. J Hematol Oncol 2018;11:129.
32. Badowska-Kozakiewicz AM, Liszcz A, Sobol M, et al. Retrospective evaluation of histopathological examinations in invasive ductal breast cancer of no special type: an analysis of 691 patients. Arch Med Sci 2017;13:1408-15.
33. Kancherla V, Abdullazade S, Matter MS, et al. Genomic Analysis Revealed New Oncogenic Signatures in TP53-Mutant Hepatocellular Carcinoma. Front Genet 2018;9:2.

Cite this article as: Liu J, Li G, Guo Y, Fan N, Zang Y. The association between genomic variations and histological grade in hepatocellular carcinoma. Transl Cancer Res 2020;9(4):2424-2433. doi: 10.21037/tcr.2020.03.32

Supplementary

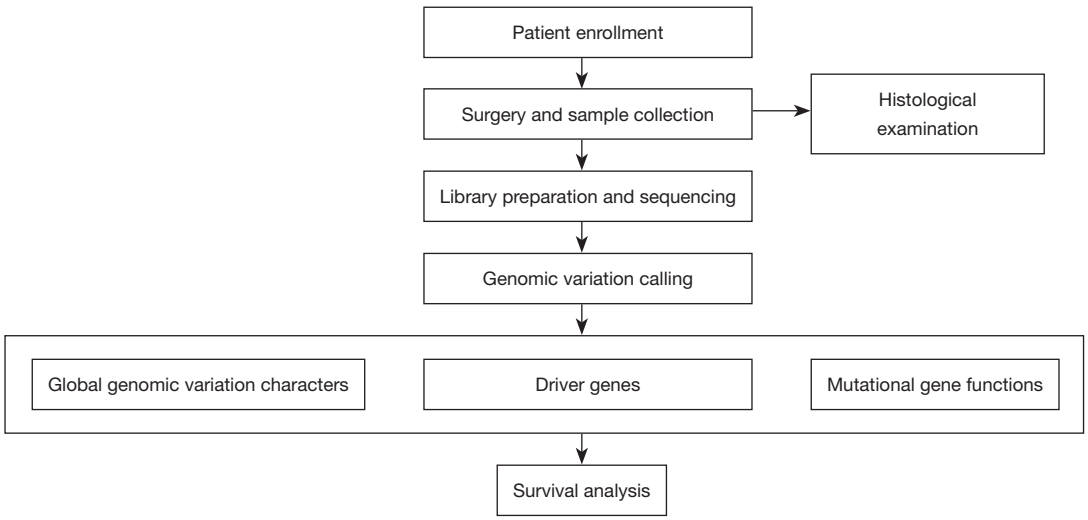

Figure S1 Workflow for this study.

Table S1 Clinical characteristics in each histological grade

Characteristics	Histological grade	
	Poor/moderate	Well
Age (mean ± SD)	54.9±15.0	60.7±12.5
Gender		
Male	358	44
Female	54	3
Stage		
I/II/III	375	43
IV	37	4
Drink		
Yes	50	7
No	362	40
Family		
Yes	92	5
No	320	42

ABCB1	CDKN2B	FGF12	LRP1B	PDCD1 (PD-1)	SMARCB1
ABL1	CDKN2C	FGF14	LRP2	PDCD1LG2	SMARCD1
ABL2	CEACAM3	FGF18	LTK	PDCD1LG2 (PD-L2)	SMO
ACVR1B	CEBPA	FGF19	LYN	PDGFB	SNCAIP
ACVR2A	CFTR	FGF2	LZTR1	PDGFRA	SND1
ADAM29	CHD2	FGF21	MACC1	PDGFRB	SOCS1
ADGRA2	CHD4	FGF23	MAF	PDK1	SOX10
AKT1	CHEK1	FGF3	MAGI2	PHF6	SOX2
AKT2	CHEK2	FGF4	MALAT1	PIK3C2B	SOX9
AKT3	CIC	FGF5	MAP2K1	PIK3C2G	SPEN
ALK	CLDN18	FGF6	MAP2K1 (MEK1)	PIK3C3	SPINK1
ALOX12B	COL1A1	FGF7	MAP2K2	PIK3CA	SPOP
AMER1	CRBN	FGF9	MAP2K2 (MEK2)	PIK3CB	SPTA1
APC	CREB3L1	FGFR1	MAP2K4	PIK3CD	SRC
APEX1	CREB3L2	FGFR2	MAP3K1	PIK3CG	SRGAP1
APOBEC3B	CREBBP	FGFR3	MAP3K13	PIK3R1	SRMS
AQP3	CRKL	FGFR4	MAP4K5	PIK3R2	SRSF2
AR	CRLF2	FGR	MAPK1	PIM1	SS18
ARAF	CSF1	FH	MCF2L	PKD2	SSX1
ARAP3	CSF1R	FLCN	MCL1	PKN1	STAG2
ARFRP1	CSF3R	FLI1	MDM2	PLA2G1B	STAT3
ARHGAP4	CSK	FLT1	MDM4	PLCG2	STAT4
ARHGAP6	CSNK1A1	FLT3	MECOM	PML	STAT6
ARHGDIA	CTCF	FLT4	MED12	PMS2	STK11
ARHGEF10	CTLA4	FOS	MEF2B	POLB	STK24
ARHGEF17	CTNNA1	FOXL2	MEN1	POLD1	SUFU
ARHGEF25	CTNNB1	FOXO1	MERTK	POLE	SUZ12
ARHGEF3	CUL3	FOXP1	MET	PPARG	SYK
ARID1A	CUL4A	FRS2	MGMT	PPP2R1A	TAF1
ARID1B	CXCR4	FUBP1	MITF	PPP2R2A	TBX3
ARID2	CYLD	FUS	MKNK1	PRDM1	TCF3
ASXL1	CYP17A1	FYN	MLH1	PREX2	TCF7L2
ATF1	CYP2D6	GABRA6	MPL	PRKACA	TEK
ATM	DAXX	GATA1	MR1	PRKAR1A	TERC
ATR	DDR1	GATA2	MRE11	PRKCI	TERT
ATRX	DDR2	GATA3	MS4A1	PRKDC	TET1
AURKA	DEF6	GATA4	MSH2	PRPF38B	TET2
AURKB	DICER1	GATA6	MSH3	PRSS1	TET3
AXIN1	DIS3	GID4	MSH6	PRSS8	TFE3
AXIN2	DLC1	GLI1	MST1R	PTCH1	TFEB
AXL	DNMT3A	GLI2	MTAP	PTEN	TGFBR1
B2M	DNMT3B	GLI3	MTG1	PTK2	TGFBR2
BAP1	DOT1L	GNA11	MTOR	PTK6	TIE1
BARD1	DPYD	GNA13	MUC16	PTPN11	TIPARP
BCL2	DYNLL1	GNAQ	MUTYH	PTPRO	TLX1
BCL2L1	ECT2	GNAS	MYB	QKI	TMPRSS2
BCL2L11 (BIM)	EED	GRIN2A	MYC	RAC1	TNFAIP3
BCL2L2	EGF	GRM3	MYCL	RAD17	TNFRSF14
BCL6	EGFR	GSK3B	MYCN	RAD21	TNFSF11
BCL7A	EMSY	GSTP1	MYD88	RAD50	TNFSF13B
BCOR	EP300	H2AFX	MYH11	RAD51	TNK2
BCORL1	EPCAM	H3F3A	MYOD1	RAD51B	TOP1
BCR	EPHA2	HCK	NAB2	RAD51C	TOP2A
BIRC3	EPHA3	HDAC1	NBN	RAD51D	TP53
BIRC5	EPHA5	HDAC9	NCOA2	RAD52	TP63
BLK	EPHA6	HGF	NCOR1	RAD54B	TPMT
BLM	EPHA7	HLA-A	NEK11	RAD54L	TRAF7
BMPR1A	EPHA8	HMGA2	NET1	RAF1	TRIO
BMX	EPHB1	HNF1A	NF1	RANBP2	TSC1
BRAF	EPHB4	HRAS	NF2	RARA	TSC2
BRCA1	ERBB2	HSD3B1	NFE2L2	RB1	TSHR
BRCA2	ERBB2 (HER2)	HSP90AA1	NFIB	RBM10	TSPAN1
BRD4	ERBB3	HTATIP2	NFKBIA	RECQL	TSPAN31
BRIP1	ERBB4	ID3	NKX2-1	RECQL4	TYK2
BTG1	ERCC1	IDH1	NOTCH1	REL	TYRO3
BTG2	ERCC4	IDH2	NOTCH2	RELA	U2AF1
BTK	ERCC5	IGF1R	NOTCH3	RELB	UGT1A1
CALR	ERG	IGF2	NOTCH4	RET	USP6
CAMTA1	ERRFI1	IKBKE	NPM1	REV3L	VEGFA
CARD11	ESR1	IKZF1	NR4A3	RHBDF2	VGLL3
CASP8	ESR1(ER)	IL7R	NRAS	RHOA	VHL
CBFB	ETV1	INHBA	NRG1	RICTOR	WEE1
CBL	ETV4	INPP4B	NRG3	RIT1	WEE2
CCND1	ETV5	IRF1	NSD1	RNF43	WISP3
CCND2	ETV6	IRF2	NSD2	ROCK1	WRN
CCND3	EWSR1	IRF4	NT5C2	ROCK2	WT1
CCNE1	EWSR1 (EWS)	IRS2	NTHL1	ROS1	XIAP
CD1A	EZH2	ITK	NTRK1	RPTOR	XPO1
CD1B	EZR	JAK1	NTRK2	RSPO2	XRCC2
CD1C	FAM135B	JAK2	NTRK3	RUNX1	XRCC3
CD1D	FAM46C	JAK3	NUP88	RUNX1T1	YAP1
CD1E	FANCA	JUN	NUP93	RXRA	YES1
CD22	FANCC	KAT6A	NUTM1	SDC4	YWHAE
CD274	FANCD2	KDM5A	OBSCN	SDHA	ZBTB2
CD274 (PD-L1)	FANCE	KDM5B	P2RY8	SDHB	ZNF217
CD36	FANCF	KDM5C	PAK1	SDHC	ZNF703
CD70	FANCG	KDM6A	PAK3	SDHD	ZNF750
CD74	FANCL	KDR	PALB2	SETBP1	ZRSR2
CD79A	FANCM	KEAP1	PARK2	SETD2	
CD79B	FARP1	KEL	PARP1	SF3B1	
CDC42	FAS	KIT	PARP2	SGK1	
CDC73	FAT1	KLHL6	PARP3	SIK1	
CDH1	FAT3	KMT2A	PARP4	SKP2	
CDK12	FAT4	KMT2C	PAX3	SLC34A2	
CDK4	FBXO31	KMT2D	PAX5	SLC6A2	
CDK6	FBXW7	KRAS	PAX7	SLIT2	
CDK8	FEN1	LCK	PBRM1	SMAD2	
CDKN1A	FEV	LIMK1	PBX1	SMAD3	
CDKN1B	FGF1	LMO1	PCA3	SMAD4	
CDKN2A	FGF10	LRP1	PDCD1	SMARCA4	

Figure S2 The gene list of the targeted sequencing.

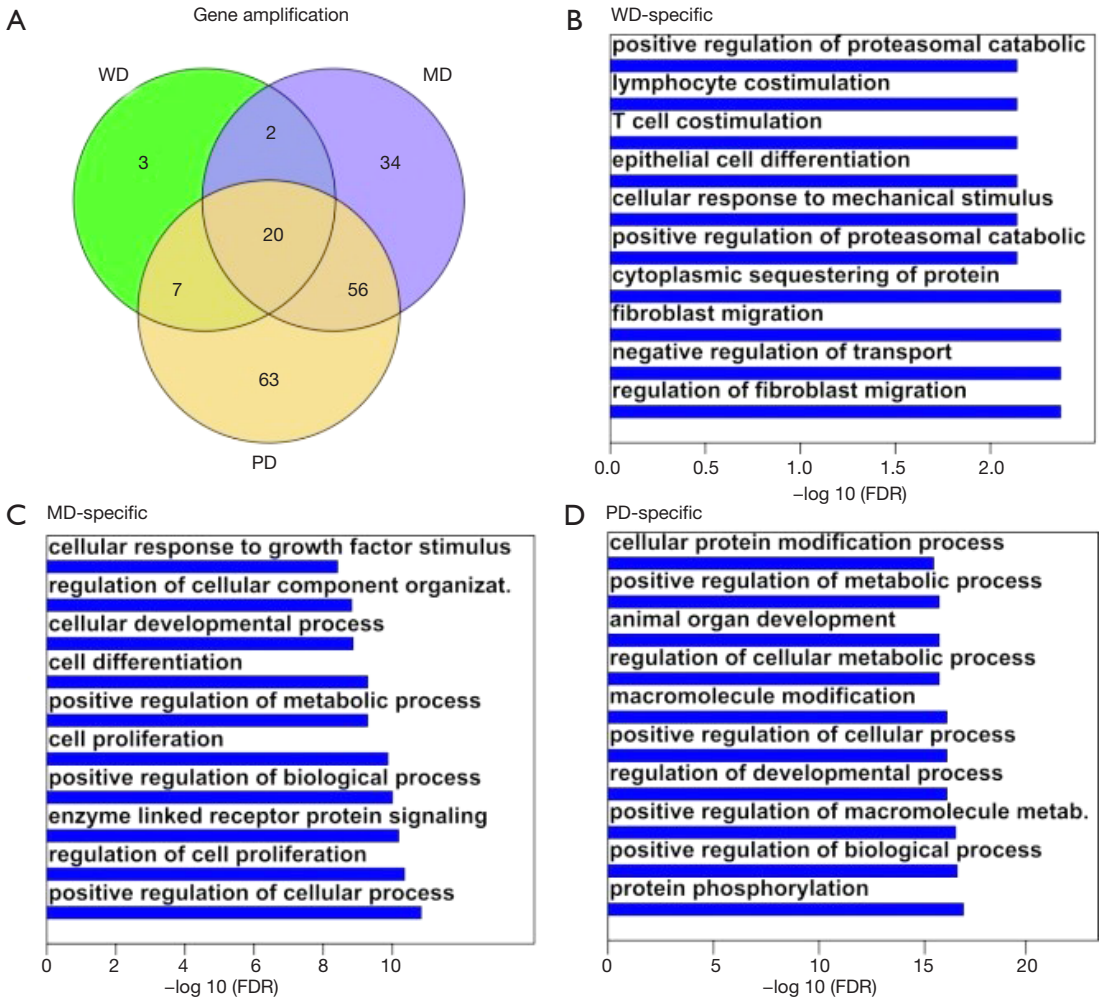

Figure S3 Gene amplification difference between different grades. (A) The gene amplification overlaps between three HGs for substitution/indel/truncation; (B) the enriched biological processes for well differentiated tumors; (C) the enriched biological processes for moderately differentiated tumors; (D) the enriched biological processes for poorly differentiated tumors. The length of the blue bar indicates the negative log transformed false discover rate (FDR). WD, well differentiated; MD, moderately differentiated; PD, poorly differentiated.

Table S2 The HG-specific biological processes

GOID	P values_adjusted	go_terms	Dataset	HG-specific
GO:0001525	1.264E-06	Angiogenesis	ZB	PD
GO:0036092	1.584E-05	Phosphatidylinositol-3-phosphate biosynthetic process	MSKCC	PD
GO:0006661	9.918E-05	Phosphatidylinositol biosynthetic process	MSKCC	PD
GO:0006650	0.0002442	Glycerophospholipid metabolic process	ZB	PD
GO:0036092	0.000248	Phosphatidylinositol-3-phosphate biosynthetic process	ZB	PD
GO:1902751	0.0002485	Positive regulation of cell cycle G2/M phase transition	ZB	PD
GO:0006650	0.0003463	Glycerophospholipid metabolic process	MSKCC	PD
GO:0006661	0.0007599	Phosphatidylinositol biosynthetic process	ZB	PD
GO:0006644	0.000767	Phospholipid metabolic process	ZB	PD
GO:0008584	0.0008151	Male gonad development	MSKCC	PD
GO:0046546	0.0008151	Development of primary male sexual characteristics	MSKCC	PD
GO:0006644	0.0010525	Phospholipid metabolic process	MSKCC	PD
GO:0046474	0.0010952	Glycerophospholipid biosynthetic process	MSKCC	PD
GO:0090218	0.0015026	Positive regulation of lipid kinase activity	MSKCC	PD
GO:0045017	0.0018219	Glycerolipid biosynthetic process	MSKCC	PD
GO:0019637	0.0019276	Organophosphate metabolic process	ZB	PD
GO:0007126	0.002289	Meiotic nuclear division	ZB	PD
GO:0008654	0.0023611	Phospholipid biosynthetic process	MSKCC	PD
GO:0043551	0.0026075	Regulation of phosphatidylinositol 3-kinase activity	MSKCC	PD
GO:1903046	0.0027839	Meiotic cell cycle process	ZB	PD
GO:1903727	0.0027864	Positive regulation of phospholipid metabolic process	MSKCC	PD
GO:0001525	0.0030352	Angiogenesis	MSKCC	PD
GO:0010518	0.0032304	Positive regulation of phospholipase activity	ZB	PD
GO:0030855	0.0040562	Epithelial cell differentiation	MSKCC	PD
GO:0035272	0.0042767	Exocrine system development	MSKCC	PD
GO:0043550	0.0042767	Regulation of lipid kinase activity	MSKCC	PD
GO:1902749	0.0046541	Regulation of cell cycle G2/M phase transition	MSKCC	PD
GO:0048146	0.0049414	Positive regulation of fibroblast proliferation	MSKCC	PD
GO:0033008	0.0050369	Positive regulation of mast cell activation involved in immune response	ZB	PD
GO:0043306	0.0050369	Positive regulation of mast cell degranulation	ZB	PD
GO:0046474	0.0050474	Glycerophospholipid biosynthetic process	ZB	PD
GO:0051321	0.0051928	Meiotic cell cycle	ZB	PD
GO:0043269	0.0052714	Regulation of ion transport	MSKCC	PD
GO:0014068	0.0059387	Positive regulation of phosphatidylinositol 3-kinase signaling	ZB	PD
GO:0033008	0.0062257	Positive regulation of mast cell activation involved in immune response	MSKCC	PD
GO:0043306	0.0062257	Positive regulation of mast cell degranulation	MSKCC	PD
GO:0033005	0.0066599	Positive regulation of mast cell activation	ZB	PD
GO:0045017	0.0071944	Glycerolipid biosynthetic process	ZB	PD
GO:0044839	0.0072853	Cell cycle G2/M phase transition	MSKCC	PD
GO:0014068	0.0073914	Positive regulation of phosphatidylinositol 3-kinase signaling	MSKCC	PD
GO:0002888	0.0080025	Positive regulation of myeloid leukocyte mediated immunity	ZB	PD
GO:0043302	0.0080025	Positive regulation of leukocyte degranulation	ZB	PD
GO:0033005	0.0082744	Positive regulation of mast cell activation	MSKCC	PD
GO:0008654	0.0087335	Phospholipid biosynthetic process	ZB	PD
GO:0034109	0.0088759	Homotypic cell-cell adhesion	ZB	PD
GO:0030855	0.0089828	Epithelial cell differentiation	ZB	PD
GO:1902751	0.0091779	Positive regulation of cell cycle G2/M phase transition	MSKCC	PD
GO:0006629	0.0093471	Lipid metabolic process	MSKCC	PD
GO:0008610	0.0100358	Lipid biosynthetic process	MSKCC	PD
GO:0002888	0.0100358	Positive regulation of myeloid leukocyte mediated immunity	MSKCC	PD
GO:0043302	0.0100358	Positive regulation of leukocyte degranulation	MSKCC	PD
GO:0034109	0.0114927	Homotypic cell-cell adhesion	MSKCC	PD
GO:0051656	0.0119185	Establishment of organelle localization	ZB	PD
GO:0043269	0.0125078	Regulation of ion transport	ZB	PD
GO:0060735	0.0129404	Regulation of eif2 alpha phosphorylation by dsRNA	ZB	PD
GO:0042102	0.0130323	Positive regulation of T cell proliferation	ZB	PD
GO:0030178	0.0141809	Negative regulation of Wnt signaling pathway	ZB	PD
GO:0006629	0.0150464	Lipid metabolic process	ZB	PD
GO:0051656	0.0165508	Establishment of organelle localization	MSKCC	PD
GO:0060735	0.0165508	Regulation of eif2 alpha phosphorylation by dsRNA	MSKCC	PD
GO:0007126	0.0170219	Meiotic nuclear division	MSKCC	PD
GO:0042102	0.0174305	Positive regulation of T cell proliferation	MSKCC	PD
GO:0090218	0.0181076	Positive regulation of lipid kinase activity	ZB	PD
GO:0032885	0.0187746	Regulation of polysaccharide biosynthetic process	ZB	PD
GO:0030178	0.0195602	Negative regulation of Wnt signaling pathway	MSKCC	PD
GO:1903046	0.0198476	Meiotic cell cycle process	MSKCC	PD
GO:0008610	0.020913	Lipid biosynthetic process	ZB	PD
GO:0032752	0.0213557	Positive regulation of interleukin-3 production	ZB	PD
GO:0042223	0.0213557	Interleukin-3 biosynthetic process	ZB	PD
GO:0043366	0.0213557	Beta selection	ZB	PD
GO:0045399	0.0213557	Regulation of interleukin-3 biosynthetic process	ZB	PD
GO:0045401	0.0213557	Positive regulation of interleukin-3 biosynthetic process	ZB	PD
GO:0007257	0.0216117	Activation of JUN kinase activity	ZB	PD
GO:0032881	0.0216117	Regulation of polysaccharide metabolic process	ZB	PD
GO:1902749	0.0218429	Regulation of cell cycle G2/M phase transition	ZB	PD
GO:0044839	0.0237717	Cell cycle G2/M phase transition	ZB	PD
GO:0033003	0.0243556	Regulation of mast cell activation	ZB	PD
GO:0043551	0.0243556	Regulation of phosphatidylinositol 3-kinase activity	ZB	PD
GO:1903727	0.0252945	Positive regulation of phospholipid metabolic process	ZB	PD
GO:0032885	0.0253146	Regulation of polysaccharide biosynthetic process	MSKCC	PD
GO:0009409	0.0262411	Response to cold	ZB	PD
GO:1903307	0.0262411	Positive regulation of regulated secretory pathway	ZB	PD
GO:0032752	0.0274151	Positive regulation of interleukin-3 production	MSKCC	PD
GO:0042223	0.0274151	Interleukin-3 biosynthetic process	MSKCC	PD
GO:0043366	0.0274151	Beta selection	MSKCC	PD
GO:0045399	0.0274151	Regulation of interleukin-3 biosynthetic process	MSKCC	PD
GO:0045401	0.0274151	Positive regulation of interleukin-3 biosynthetic process	MSKCC	PD
GO:0008584	0.0282742	Male gonad development	ZB	PD
GO:0046546	0.0282742	Development of primary male sexual characteristics	ZB	PD
GO:0002351	0.0282742	Serotonin production involved in inflammatory response	ZB	PD
GO:0002442	0.0282742	Serotonin secretion involved in inflammatory response	ZB	PD
GO:0002554	0.0282742	Serotonin secretion by platelet	ZB	PD
GO:0032252	0.0282742	Secretory granule localization	ZB	PD
GO:0032672	0.0282742	Regulation of interleukin-3 production	ZB	PD
GO:0045425	0.0282742	Positive regulation of granulocyte macrophage colony-stimulating factor biosynthetic process	ZB	PD
GO:0045588	0.0282742	Positive regulation of gamma-delta T cell differentiation	ZB	PD
GO:1901843	0.0282742	Positive regulation of high voltage-gated calcium channel activity	ZB	PD
GO:0007257	0.0285333	Activation of JUN kinase activity	MSKCC	PD
GO:0032881	0.0285333	Regulation of polysaccharide metabolic process	MSKCC	PD
GO:0042129	0.0307477	Regulation of T cell proliferation	ZB	PD
GO:0051321	0.0309104	Meiotic cell cycle	MSKCC	PD
GO:0035272	0.0318221	Exocrine system development	ZB	PD
GO:0043550	0.0318221	Regulation of lipid kinase activity	ZB	PD
GO:0033003	0.0322116	Regulation of mast cell activation	MSKCC	PD
GO:0048146	0.0343113	Positive regulation of fibroblast proliferation	ZB	PD
GO:0010897	0.0343113	Negative regulation of triglyceride catabolic process	ZB	PD
GO:0032632	0.0343113	Interleukin-3 production	ZB	PD
GO:0045423	0.0343113	Regulation of granulocyte macrophage colony-stimulating factor biosynthetic process	ZB	PD
GO:0060699	0.0343113	Regulation of endoribonuclease activity	ZB	PD
GO:0007405	0.0343407	Neuroblast proliferation	ZB	PD
GO:0009409	0.0344727	Response to cold	MSKCC	PD
GO:1903307	0.0344727	Positive regulation of regulated secretory pathway	MSKCC	PD
GO:0002351	0.0359801	Serotonin production involved in inflammatory response	MSKCC	PD
GO:0002442	0.0359801	Serotonin secretion involved in inflammatory response	MSKCC	PD
GO:0002554	0.0359801	Serotonin secretion by platelet	MSKCC	PD
GO:0032252	0.0359801	Secretory granule localization	MSKCC	PD
GO:0032672	0.0359801	Regulation of interleukin-3 production	MSKCC	PD
GO:0045425	0.0359801	Positive regulation of granulocyte macrophage colony-stimulating factor biosynthetic process	MSKCC	PD
GO:0045588	0.0359801	Positive regulation of gamma-delta T cell differentiation	MSKCC	PD
GO:1901843	0.0359801	Positive regulation of high voltage-gated calcium channel activity	MSKCC	PD
GO:0010518	0.040339	Positive regulation of phospholipase activity	MSKCC	PD
GO:0042129	0.0411271	Regulation of T cell proliferation	MSKCC	PD
GO:0010897	0.0437818	Negative regulation of triglyceride catabolic process	MSKCC	PD
GO:0032632	0.0437818	Interleukin-3 production	MSKCC	PD
GO:0045423	0.0437818	Regulation of granulocyte macrophage colony-stimulating factor biosynthetic process	MSKCC	PD
GO:0060699	0.0437818	Regulation of endoribonuclease activity	MSKCC	PD
GO:0007405	0.0450633	Neuroblast proliferation	MSKCC	PD
GO:0019637	0.045281	Organophosphate metabolic process	MSKCC	PD
GO:0042542	1.365E-07	Response to hydrogen peroxide	MSKCC	MD
GO:0014812	1.111E-06	Muscle cell migration	MSKCC	MD
GO:0042493	1.147E-06	Response to drug	MSKCC	MD
GO:1901652	1.569E-06	Response to peptide	ZB	MD
GO:0044092	1.981E-06	Negative regulation of molecular function	ZB	MD
GO:0043434	5.246E-06	Response to peptide hormone	ZB	MD
GO:0000302	1.172E-05	Response to reactive oxygen species	MSKCC	MD
GO:0034504	1.315E-05	Protein localization to nucleus	MSKCC	MD
GO:0033365	1.481E-05	Protein localization to organelle	MSKCC	MD
GO:0070301	2.532E-05	Cellular response to hydrogen peroxide	MSKCC	MD
GO:0009607	3.12E-05	Response to biotic stimulus	MSKCC	MD
GO:0034614	4.066E-05	Cellular response to reactive oxygen species	MSKCC	MD
GO:1904705	4.887E-05	Regulation of vascular smooth muscle cell proliferation	MSKCC	MD
GO:1990874	4.887E-05	Vascular smooth muscle cell proliferation	MSKCC	MD
GO:0003279	6.629E-05	Cardiac septum development	MSKCC	MD
GO:0051707	6.996E-05	Response to other organism	MSKCC	MD
GO:0043207	7.068E-05	Response to external biotic stimulus	MSKCC	MD
GO:1901652	7.61E-05	Response to peptide	MSKCC	MD
GO:0051223	9.568E-05	Regulation of protein transport	MSKCC	MD
GO:0060411	0.0001143	Cardiac septum morphogenesis	MSKCC	MD
GO:0014909	0.0001298	Smooth muscle cell migration	MSKCC	MD
GO:0032496	0.0001321	Response to lipopolysaccharide	MSKCC	MD
GO:0045682	0.0001383	Regulation of epidermis development	MSKCC	MD
GO:0006273	0.0001448	Lagging strand elongation	MSKCC	MD
GO:0043434	0.0001755	Response to peptide hormone	MSKCC	MD
GO:0002237	0.0001807	Response to molecule of bacterial origin	MSKCC	MD
GO:0003179	0.000188	Heart valve morphogenesis	MSKCC	MD
GO:0050864	0.0002231	Regulation of B cell activation	MSKCC	MD
GO:0003170	0.0002759	Heart valve development	MSKCC	MD
GO:0051570	0.0003745	Regulation of histone H3-K9 methylation	ZB	MD
GO:0044092	0.0004357	Negative regulation of molecular function	MSKCC	MD
GO:0042100	0.0004756	B cell proliferation	MSKCC	MD
GO:0000302	0.0005009	Response to reactive oxygen species	ZB	MD
GO:1904019	0.0005234	Epithelial cell apoptotic process	MSKCC	MD
GO:0006266	0.0005342	DNA ligation	ZB	MD
GO:0034614	0.00056	Cellular response to reactive oxygen species	ZB	MD
GO:2001242	0.0005685	Regulation of intrinsic apoptotic signaling pathway	MSKCC	MD
GO:0046879	0.0006353	Hormone secretion	MSKCC	MD
GO:0006271	0.0006777	DNA strand elongation involved in DNA replication	MSKCC	MD
GO:0003205	0.0007089	Cardiac chamber development	MSKCC	MD
GO:0003007	0.0007878	Heart morphogenesis	MSKCC	MD
GO:0009914	0.0008096	Hormone transport	MSKCC	MD
GO:0034504	0.0008947	Protein localization to nucleus	ZB	MD
GO:0051567	0.000944	Histone H3-K9 methylation	ZB	MD
GO:0030888	0.001	Regulation of B cell proliferation	MSKCC	MD
GO:0032611	0.001	Interleukin-1 beta production	MSKCC	MD
GO:0033157	0.001093	Regulation of intracellular protein transport	ZB	MD
GO:1902042	0.001286	Negative regulation of extrinsic apoptotic signaling pathway via death domain receptors	ZB	MD
GO:0050852	0.0012901	T cell receptor signaling pathway	MSKCC	MD
GO:0006266	0.0012907	DNA ligation	MSKCC	MD
GO:0032845	0.0013576	Negative regulation of homeostatic process	MSKCC	MD
GO:0003281	0.0014821	Ventricular septum development	MSKCC	MD
GO:0033143	0.0014821	Regulation of intracellular steroid hormone receptor signaling pathway	MSKCC	MD
GO:0022616	0.001571	DNA strand elongation	MSKCC	MD
GO:0071887	0.0016635	Leukocyte apoptotic process	ZB	MD
GO:1904035	0.0017433	Regulation of epithelial cell apoptotic process	MSKCC	MD
GO:0032612	0.0019145	Interleukin-1 production	MSKCC	MD
GO:0097306	0.0019363	Cellular response to alcohol	ZB	MD
GO:0034968	0.0021658	Histone lysine methylation	ZB	MD
GO:0061647	0.002279	Histone H3-K9 modification	ZB	MD
GO:0033146	0.002285	Regulation of intracellular estrogen receptor signaling pathway	MSKCC	MD
GO:0022408	0.0023527	Negative regulation of cell-cell adhesion	MSKCC	MD
GO:0033157	0.0023985	Regulation of intracellular protein transport	MSKCC	MD
GO:0051223	0.0024086	Regulation of protein transport	ZB	MD
GO:0032446	0.0024086	Protein modification by small protein conjugation	ZB	MD
GO:0051573	0.0028681	Negative regulation of histone H3-K9 methylation	ZB	MD
GO:0018022	0.0028725	Peptidyl-lysine methylation	ZB	MD
GO:0046824	0.0028725	Positive regulation of nucleocytoplasmic transport	ZB	MD
GO:0031648	0.0030756	Protein destabilization	MSKCC	MD
GO:0009636	0.0032692	Response to toxic substance	ZB	MD
GO:0006261	0.0033055	DNA-dependent DNA replication	MSKCC	MD
GO:0006273	0.0033374	Lagging strand elongation	ZB	MD
GO:0002223	0.0035118	Stimulatory C-type lectin receptor signaling pathway	ZB	MD
GO:0002220	0.0036986	Innate immune response activating cell surface receptor signaling pathway	ZB	MD
GO:0051103	0.0038896	DNA ligation involved in DNA repair	ZB	MD
GO:0003007	0.0040602	Heart morphogenesis	ZB	MD
GO:0016571	0.0042866	Histone methylation	ZB	MD
GO:0097306	0.0044943	Cellular response to alcohol	MSKCC	MD
GO:0031060	0.0045733	Regulation of histone methylation	ZB	MD
GO:0023061	0.0047426	Signal release	MSKCC	MD
GO:0051573	0.0047426	Negative regulation of histone H3-K9 methylation	MSKCC	MD
GO:0001666	0.0047462	Response to hypoxia	MSKCC	MD
GO:0006284	0.0050431	Base-excision repair	MSKCC	MD
GO:0018205	0.0051017	Peptidyl-lysine modification	ZB	MD
GO:0036293	0.0053204	Response to decreased oxygen levels	MSKCC	MD
GO:0061647	0.0053204	Histone H3-K9 modification	MSKCC	MD
GO:0006261	0.0055276	DNA-dependent DNA replication	ZB	MD
GO:2001020	0.0055567	Regulation of response to DNA damage stimulus	MSKCC	MD
GO:0032446	0.0057176	Protein modification by small protein conjugation	MSKCC	MD
GO:0014909	0.0058867	Smooth muscle cell migration	ZB	MD
GO:0070664	0.0058867	Negative regulation of leukocyte proliferation	ZB	MD
GO:0090316	0.0059508	Positive regulation of intracellular protein transport	MSKCC	MD
GO:0032651	0.0061433	Regulation of interleukin-1 beta production	MSKCC	MD
GO:0006304	0.0062479	DNA modification	MSKCC	MD
GO:0051103	0.0062941	DNA ligation involved in DNA repair	MSKCC	MD
GO:0030520	0.0064205	Intracellular estrogen receptor signaling pathway	MSKCC	MD
GO:0042093	0.0064205	T-helper cell differentiation	MSKCC	MD
GO:0045936	0.0065605	Negative regulation of phosphate metabolic process	ZB	MD
GO:0010563	0.0066057	Negative regulation of phosphorus metabolic process	ZB	MD
GO:0045604	0.0067768	Regulation of epidermal cell differentiation	MSKCC	MD
GO:0031061	0.0067822	Negative regulation of histone methylation	ZB	MD
GO:0034968	0.0067993	Histone lysine methylation	MSKCC	MD
GO:0002294	0.0071277	CD4-positive, alpha-beta T cell differentiation involved in immune response	MSKCC	MD
GO:0002287	0.0074349	alpha-beta T cell activation involved in immune response	MSKCC	MD
GO:0002293	0.0074349	alpha-beta T cell differentiation involved in immune response	MSKCC	MD
GO:0031663	0.0074349	Lipopolysaccharide-mediated signaling pathway	MSKCC	MD
GO:0038034	0.0077505	Signal transduction in absence of ligand	ZB	MD
GO:0097192	0.0077505	Extrinsic apoptotic signaling pathway in absence of ligand	ZB	MD
GO:0034284	0.0078981	Response to monosaccharide	MSKCC	MD
GO:0006271	0.0081662	DNA strand elongation involved in DNA replication	ZB	MD
GO:0046660	0.0082366	Female sex differentiation	MSKCC	MD
GO:0014812	0.008241	Muscle cell migration	ZB	MD
GO:0003283	0.0088126	Atrial septum development	ZB	MD
GO:0023019	0.0088126	Signal transduction involved in regulation of gene expression	ZB	MD
GO:0007259	0.0089793	JAK-STAT cascade	ZB	MD
GO:0097696	0.0089793	STAT cascade	ZB	MD
GO:0018022	0.0091089	Peptidyl-lysine methylation	MSKCC	MD
GO:0046824	0.0091089	Positive regulation of nucleocytoplasmic transport	MSKCC	MD
GO:0001541	0.0092698	Ovarian follicle development	MSKCC	MD
GO:0070301	0.0095041	Cellular response to hydrogen peroxide	ZB	MD
GO:0002292	0.0096977	T cell differentiation involved in immune response	MSKCC	MD
GO:1903533	0.0097929	Regulation of protein targeting	ZB	MD
GO:0006479	0.0099192	Protein methylation	ZB	MD
GO:0008213	0.0099192	Protein alkylation	ZB	MD
GO:0050852	0.0099192	T cell receptor signaling pathway	ZB	MD
GO:0032845	0.0101971	Negative regulation of homeostatic process	ZB	MD
GO:0031060	0.0104978	Regulation of histone methylation	MSKCC	MD
GO:0032652	0.0104978	Regulation of interleukin-1 production	MSKCC	MD
GO:0008625	0.0108141	Extrinsic apoptotic signaling pathway via death domain receptors	ZB	MD
GO:0032496	0.0108141	Response to lipopolysaccharide	ZB	MD
GO:0009743	0.0108748	Response to carbohydrate	MSKCC	MD
GO:0001947	0.0108748	Heart looping	MSKCC	MD
GO:0048678	0.0108748	Response to axon injury	MSKCC	MD
GO:0072091	0.0108748	Regulation of stem cell proliferation	MSKCC	MD
GO:1903533	0.0110206	Regulation of protein targeting	MSKCC	MD
GO:0002223	0.0110206	Stimulatory C-type lectin receptor signaling pathway	MSKCC	MD
GO:0031061	0.0110206	Negative regulation of histone methylation	MSKCC	MD
GO:0043367	0.0112179	CD4-positive, alpha-beta T cell differentiation	MSKCC	MD
GO:0002220	0.0115502	Innate immune response activating cell surface receptor signaling pathway	MSKCC	MD
GO:1904705	0.0117161	Regulation of vascular smooth muscle cell proliferation	ZB	MD
GO:1990874	0.0117161	Vascular smooth muscle cell proliferation	ZB	MD
GO:0042100	0.0117593	B cell proliferation	ZB	MD
GO:1904019	0.0124536	Epithelial cell apoptotic process	ZB	MD
GO:0006471	0.0125445	Protein ADP-ribosylation	ZB	MD
GO:0002237	0.0127762	Response to molecule of bacterial origin	ZB	MD
GO:0061371	0.0130477	Determination of heart left/right asymmetry	MSKCC	MD
GO:0016571	0.0132027	Histone methylation	MSKCC	MD
GO:0022616	0.0132769	DNA strand elongation	ZB	MD
GO:0008585	0.0132769	Female gonad development	ZB	MD
GO:0003143	0.0134719	Embryonic heart tube morphogenesis	MSKCC	MD
GO:0008589	0.0134719	Regulation of smoothened signaling pathway	MSKCC	MD
GO:0035710	0.0134719	CD4-positive, alpha-beta T cell activation	MSKCC	MD
GO:0070664	0.0134719	Negative regulation of leukocyte proliferation	MSKCC	MD
GO:0071301	0.0136096	Cellular response to vitamin B1	ZB	MD
GO:0090347	0.0136096	Regulation of cellular organohalogen metabolic process	ZB	MD
GO:0090348	0.0136096	Regulation of cellular organofluorine metabolic process	ZB	MD
GO:0090349	0.0136096	Negative regulation of cellular organohalogen metabolic process	ZB	MD
GO:0090350	0.0136096	Negative regulation of cellular organofluorine metabolic process	ZB	MD
GO:1904404	0.0136096	Response to formaldehyde	ZB	MD
GO:0003279	0.0136766	Cardiac septum development	ZB	MD
GO:0046545	0.0139992	Development of primary female sexual characteristics	ZB	MD
GO:0009743	0.0140538	Response to carbohydrate	ZB	MD
GO:0043086	0.0143878	Negative regulation of catalytic activity	ZB	MD
GO:0003283	0.0143938	Atrial septum development	MSKCC	MD
GO:0023019	0.0143938	Signal transduction involved in regulation of gene expression	MSKCC	MD
GO:0007389	0.015078	Pattern specification process	MSKCC	MD
GO:0006304	0.0153019	DNA modification	ZB	MD
GO:0051100	0.0154442	Negative regulation of binding	MSKCC	MD
GO:0045936	0.0155204	Negative regulation of phosphate metabolic process	MSKCC	MD
GO:0051570	0.015525	Regulation of histone H3-K9 methylation	MSKCC	MD
GO:0010563	0.01554	Negative regulation of phosphorus metabolic process	MSKCC	MD
GO:0046634	0.0155981	Regulation of alpha-beta T cell activation	MSKCC	MD
GO:0071301	0.0155981	Cellular response to vitamin B1	MSKCC	MD
GO:0090347	0.0155981	Regulation of cellular organohalogen metabolic process	MSKCC	MD
GO:0090348	0.0155981	Regulation of cellular organofluorine metabolic process	MSKCC	MD
GO:0090349	0.0155981	Negative regulation of cellular organohalogen metabolic process	MSKCC	MD
GO:0090350	0.0155981	Negative regulation of cellular organofluorine metabolic process	MSKCC	MD
GO:1904404	0.0155981	Response to formaldehyde	MSKCC	MD
GO:0033146	0.0159353	Regulation of intracellular estrogen receptor signaling pathway	ZB	MD
GO:0051051	0.0167241	Negative regulation of transport	MSKCC	MD
GO:0038034	0.0167508	Signal transduction in absence of ligand	MSKCC	MD
GO:0097192	0.0167508	Extrinsic apoptotic signaling pathway in absence of ligand	MSKCC	MD
GO:0046660	0.0191336	Female sex differentiation	ZB	MD
GO:0031648	0.01952	Protein destabilization	ZB	MD
GO:0006471	0.0196997	Protein ADP-ribosylation	MSKCC	MD
GO:0043086	0.0202833	Negative regulation of catalytic activity	MSKCC	MD
GO:0003179	0.0203264	Heart valve morphogenesis	ZB	MD
GO:0003230	0.0203264	Cardiac atrium development	ZB	MD
GO:0033365	0.0219486	Protein localization to organelle	ZB	MD
GO:0042542	0.0231473	Response to hydrogen peroxide	ZB	MD
GO:0010868	0.0231473	Negative regulation of triglyceride biosynthetic process	ZB	MD
GO:0071460	0.0231473	Cellular response to cell-matrix adhesion	ZB	MD
GO:0090345	0.0231473	Cellular organohalogen metabolic process	ZB	MD
GO:0090346	0.0231473	Cellular organofluorine metabolic process	ZB	MD
GO:0050864	0.0232449	Regulation of B cell activation	ZB	MD
GO:0044262	0.0234314	Cellular carbohydrate metabolic process	MSKCC	MD
GO:0003170	0.0234325	Heart valve development	ZB	MD
GO:0008625	0.0238195	Extrinsic apoptotic signaling pathway via death domain receptors	MSKCC	MD
GO:0043029	0.0244019	T cell homeostasis	ZB	MD
GO:0046825	0.0252439	Regulation of protein export from nucleus	ZB	MD
GO:0018205	0.0254654	Peptidyl-lysine modification	MSKCC	MD
GO:0090316	0.0255328	Positive regulation of intracellular protein transport	ZB	MD
GO:0022408	0.0260472	Negative regulation of cell-cell adhesion	ZB	MD
GO:0006284	0.0260472	Base-excision repair	ZB	MD
GO:0010883	0.0260472	Regulation of lipid storage	ZB	MD
GO:0007259	0.0262577	JAK-STAT cascade	MSKCC	MD
GO:0097696	0.0262577	STAT cascade	MSKCC	MD
GO:0051567	0.0262577	Histone H3-K9 methylation	MSKCC	MD
GO:0010868	0.0262577	Negative regulation of triglyceride biosynthetic process	MSKCC	MD
GO:0071460	0.0262577	Cellular response to cell-matrix adhesion	MSKCC	MD
GO:0090345	0.0262577	Cellular organohalogen metabolic process	MSKCC	MD
GO:0090346	0.0262577	Cellular organofluorine metabolic process	MSKCC	MD
GO:0044262	0.0265122	Cellular carbohydrate metabolic process	ZB	MD
GO:0042493	0.0271005	Response to drug	ZB	MD
GO:0006479	0.0275738	Protein methylation	MSKCC	MD
GO:0008213	0.0275738	Protein alkylation	MSKCC	MD
GO:0008585	0.0277022	Female gonad development	MSKCC	MD
GO:0051100	0.029382	Negative regulation of binding	ZB	MD
GO:0032651	0.0295013	Regulation of interleukin-1 beta production	ZB	MD
GO:0043525	0.0295013	Positive regulation of neuron apoptotic process	ZB	MD
GO:0051055	0.0295013	Negative regulation of lipid biosynthetic process	ZB	MD
GO:0007389	0.0295013	Pattern specification process	ZB	MD
GO:0023061	0.0295013	Signal release	ZB	MD
GO:0030520	0.0295013	Intracellular estrogen receptor signaling pathway	ZB	MD
GO:0042093	0.0295013	T-helper cell differentiation	ZB	MD
GO:0009822	0.0295013	Alkaloid catabolic process	ZB	MD
GO:0010266	0.0295013	Response to vitamin B1	ZB	MD
GO:0033076	0.0295013	Isoquinoline alkaloid metabolic process	ZB	MD
GO:0071494	0.0295013	Cellular response to UV-C	ZB	MD
GO:0098760	0.0295013	Response to interleukin-7	ZB	MD
GO:0098761	0.0295013	Cellular response to interleukin-7	ZB	MD
GO:1990785	0.0295013	Response to water-immersion restraint stress	ZB	MD
GO:0071887	0.029714	Leukocyte apoptotic process	MSKCC	MD
GO:0045604	0.0298719	Regulation of epidermal cell differentiation	ZB	MD
GO:0046545	0.0305378	Development of primary female sexual characteristics	MSKCC	MD
GO:1902042	0.0306947	Negative regulation of extrinsic apoptotic signaling pathway via death domain receptors	MSKCC	MD
GO:0002294	0.0309829	CD4-positive, alpha-beta T cell differentiation involved in immune response	ZB	MD
GO:0002287	0.0320739	alpha-beta T cell activation involved in immune response	ZB	MD
GO:0002293	0.0320739	alpha-beta T cell differentiation involved in immune response	ZB	MD
GO:0031663	0.0320739	Lipopolysaccharide-mediated signaling pathway	ZB	MD
GO:0003230	0.0321242	Cardiac atrium development	MSKCC	MD
GO:2001242	0.0323501	Regulation of intrinsic apoptotic signaling pathway	ZB	MD
GO:0051051	0.0324454	Negative regulation of transport	ZB	MD
GO:0051707	0.0338559	Response to other organism	ZB	MD
GO:0043207	0.033997	Response to external biotic stimulus	ZB	MD
GO:0009822	0.0354738	Alkaloid catabolic process	MSKCC	MD
GO:0010266	0.0354738	Response to vitamin B1	MSKCC	MD
GO:0033076	0.0354738	Isoquinoline alkaloid metabolic process	MSKCC	MD
GO:0071494	0.0354738	Cellular response to UV-C	MSKCC	MD
GO:0098760	0.0354738	Response to interleukin-7	MSKCC	MD
GO:0098761	0.0354738	Cellular response to interleukin-7	MSKCC	MD
GO:1990785	0.0354738	Response to water-immersion restraint stress	MSKCC	MD
GO:0003205	0.0358613	Cardiac chamber development	ZB	MD
GO:0001541	0.0363016	Ovarian follicle development	ZB	MD
GO:0007089	0.0363016	Traversing start control point of mitotic cell cycle	ZB	MD
GO:0010989	0.0363016	Negative regulation of low-density lipoprotein particle clearance	ZB	MD
GO:0014042	0.0363016	Positive regulation of neuron maturation	ZB	MD
GO:0035799	0.0363016	Ureter maturation	ZB	MD
GO:0042997	0.0363016	Negative regulation of Golgi to plasma membrane protein transport	ZB	MD
GO:0070427	0.0363016	Nucleotide-binding oligomerization domain containing 1 signaling pathway	ZB	MD
GO:2000048	0.0363016	Negative regulation of cell-cell adhesion mediated by cadherin	ZB	MD
GO:0046879	0.0364954	Hormone secretion	ZB	MD
GO:0002292	0.0371894	T cell differentiation involved in immune response	ZB	MD
GO:0030888	0.0371894	Regulation of B cell proliferation	ZB	MD
GO:0032611	0.0371894	Interleukin-1 beta production	ZB	MD
GO:0043029	0.0386747	T cell homeostasis	MSKCC	MD
GO:0032652	0.0392552	Regulation of interleukin-1 production	ZB	MD
GO:2001020	0.039929	Regulation of response to DNA damage stimulus	ZB	MD
GO:0046825	0.0400926	Regulation of protein export from nucleus	MSKCC	MD
GO:0001947	0.040316	Heart looping	ZB	MD
GO:0048678	0.040316	Response to axon injury	ZB	MD
GO:0072091	0.040316	Regulation of stem cell proliferation	ZB	MD
GO:0009914	0.0407189	Hormone transport	ZB	MD
GO:0009607	0.0410816	Response to biotic stimulus	ZB	MD
GO:0043367	0.0414048	CD4-positive, alpha-beta T cell differentiation	ZB	MD
GO:0010883	0.0416577	Regulation of lipid storage	MSKCC	MD
GO:0007089	0.0432135	Traversing start control point of mitotic cell cycle	MSKCC	MD
GO:0010989	0.0432135	Negative regulation of low-density lipoprotein particle clearance	MSKCC	MD
GO:0014042	0.0432135	Positive regulation of neuron maturation	MSKCC	MD
GO:0035799	0.0432135	Ureter maturation	MSKCC	MD
GO:0042997	0.0432135	Negative regulation of Golgi to plasma membrane protein transport	MSKCC	MD
GO:0070427	0.0432135	Nucleotide-binding oligomerization domain containing 1 signaling pathway	MSKCC	MD
GO:2000048	0.0432135	Negative regulation of cell-cell adhesion mediated by cadherin	MSKCC	MD
GO:0003281	0.0437357	Ventricular septum development	ZB	MD
GO:0033143	0.0437357	Regulation of intracellular steroid hormone receptor signaling pathway	ZB	MD
GO:0060411	0.0437357	Cardiac septum morphogenesis	ZB	MD
GO:0061371	0.0447239	Determination of heart left/right asymmetry	ZB	MD
GO:0009636	0.0455879	Response to toxic substance	MSKCC	MD
GO:0003143	0.0456721	Embryonic heart tube morphogenesis	ZB	MD
GO:0008589	0.0456721	Regulation of smoothened signaling pathway	ZB	MD
GO:0035710	0.0456721	CD4-positive, alpha-beta T cell activation	ZB	MD
GO:0001666	0.0462698	Response to hypoxia	ZB	MD
GO:0043525	0.0463606	Positive regulation of neuron apoptotic process	MSKCC	MD
GO:0051055	0.0463606	Negative regulation of lipid biosynthetic process	MSKCC	MD
GO:0045682	0.0465784	Regulation of epidermis development	ZB	MD
GO:1904035	0.0465784	Regulation of epithelial cell apoptotic process	ZB	MD
GO:0034284	0.0473956	Response to monosaccharide	ZB	MD
GO:0032612	0.0473956	Interleukin-1 production	ZB	MD
GO:0036293	0.047653	Response to decreased oxygen levels	ZB	MD
GO:0046634	0.0493719	Regulation of alpha-beta T cell activation	ZB	MD
GO:1905005	0.0303648	Regulation of epithelial to mesenchymal transition involved in endocardial cushion formation	ZB	WD
GO:0003198	0.0462411	Epithelial to mesenchymal transition involved in endocardial cushion formation	ZB	WD
GO:0034110	0.0498585	Regulation of homotypic cell-cell adhesion	ZB	WD
GO:1905005	0.027475	Regulation of epithelial to mesenchymal transition involved in endocardial cushion formation	MSKCC	WD
GO:0003198	0.0414965	Epithelial to mesenchymal transition involved in endocardial cushion formation	MSKCC	WD
GO:0034110	0.0441837	Regulation of homotypic cell-cell adhesion	MSKCC	WD

Note: dataset, our dataset was named ZB. PD, poor differentiated; MD, moderate differentiated; WD, well differentiated.